ELSEVIER

Journal of Chromatography A, 763 (1997) 71–90

JOURNAL OF CHROMATOGRAPHY A

Comparative studies on the isothermal characteristics of proteins adsorbed under batch equilibrium conditions to ion-exchange, immobilised metal ion affinity and dye affinity matrices with different ionic strength and temperature conditions[1]

Gerard M.S. Finette, Qui-Ming Mao, Milton T.W. Hearn*

Centre for Bioprocess Technology, Department of Biochemistry and Molecular Biology, Monash University, Wellington Road, Clayton, Victoria 3168, Australia

Abstract

In these investigations, the influence of a range of experimental parameters on the isothermal characteristics of hen egg white lysozyme (HEWL) and human serum albumin (HSA) adsorbed to several different adsorbents has been examined. The adsorbents were selected to encompass the same basic types of silica support matrices, but with the ligand properties and surface characteristics adjusted so that the dominant mode of interaction between the protein and the ligand involved either electrostatic binding (i.e. as ion-exchange interactions with polyaspartic acid immobilised onto glycidoxypropyl-modified Fractosil 1000), mixed-mode binding with both hydrophobic and electrostatic effects contributing to the protein–ligand interaction (i.e. as dye-affinity interactions with Cibacron Blue F3G-A immobilised onto Lichroprep DIOL or onto glycidoxypropyl-modified Fractosil 1000), or lone pair coordination binding (i.e. as immobilised metal ion affinity (IMAC) interactions with Cu^{2+} ions complexed with iminodiacetic acid immobilised onto glycidoxypropyl-modified Fractosil 1000). In each case, the adsorbents exhibited similar ligand densities and had the same particle size ranges and silica surface pretreatment. The effect of the ionic strength of the adsorption buffer and temperature on the isothermal adsorption behaviour under batch equilibrium binding conditions of the two test proteins were determined. Consistent with previous observations with soft gel ion exchangers and triazine dye-based adsorbents that are used in packed bed chromatographic systems, the capacities of the silica-based ion-exchange adsorbents, as well as the Cibacron Blue F3G-A dye affinity adsorbents, for both HSA and HEWL were reduced as the salt concentration was increased under batch equilibrium binding conditions. Moreover, with both of these classes of adsorbents, as the ionic strength was increased under constant temperature conditions, the isothermal adsorption dependencies progressively approximated more closely a Langmuirean model of independent binding site interactions, typical of a mono-layer binding process. In contrast, with the silica-based immobilised metal ion affinity adsorbents as the ionic strength was increased the adsorption behaviour appeared to follow a Freundlich model, indicative of positive cooperativity in the binding process. In parallel experiments, the effect of changes in temperature under iso-ionic strength conditions was examined. With increasing temperature, different patterns of isothermal adsorption behaviour for both test proteins were observed, with the magnitude of these trends depending on the type of interaction involved between the immobilised ligand and the protein. Utilising first order Van 't Hoff relationships to analyse the experimental data for these protein–ligand interactions, the apparent changes in enthalpy and entropy for these interactions have been derived from the dependency of the change in the apparent Gibbs free energy on $1/T$.

*Corresponding author.

[1]Part CLXX of the series High-performance liquid chromatography of amino acids, peptides and proteins. For Part CLXIX see Ref. [43].

PII S0021-9673(96)00956-9

Keywords: Stationary phases, LC; Thermodynamic parameters; Adsorption isotherms; Affinity adsorbents; Proteins; Lysozyme; Albumin

1. Introduction

In recent years, the availability of improved silica-based adsorbents of different ligand selectivities has provided an important avenue for increasing throughput and productivity in preparative protein purification [1–3]. Because silica-based adsorbents tend to be more mechanically stable and can now be economically manufactured in particle and pore size ranges suitable for preparative applications, surface-modified silicas are increasingly finding application in industrial and process settings. Porous reversed-phase silicas with particle sizes of $\geq$16 μm, in particular, have found important commercial niches for process applications with synthetic and recombinant peptides and polypeptides [4–6], whilst increasingly, silica-based ion-exchange and immobilised metal ion affinity chromatographic adsorbents are attracting interest for process purification of proteins [1,2,7].

As a consequence of these developments, it has increasingly been recognised that the more extensive usage of silica-based adsorbents of large particle size for process applications with proteins and other high-molecular-mass biomacromolecules will be dependent on several limitations being overcome. Besides the constraint imposed by the chemical instability of most types of preparative grades of porous silica to pH values greater than pH 8.0, from a process point of view, the greatest single limitation to their usage still remains the paucity of information on the adsorption behaviour of proteins under preparative loading regimes and, in particular, how the specific adsorption isotherms of multi-component mixtures will change in response to variations in (i) the physical (particle size and distribution, pore size and distribution) and surface (silica type in terms of relative abundance of the different classes of silanol groups, surface acidity, trace metal ion content, and the ligand type, density or distribution) characteristics of the adsorbent; (ii) the composition of the adsorption and elution buffer(s) and (iii) key thermodynamic parameters such as temperature and phase ratio.

Considerable progress in the stabilisation of porous silicas suitable for process applications has been achieved in recent years, either through improvement in the surface modification chemistries associated with the immobilisation of the specific ligand and the masking (or end-capping) of the residual underlying silanol effects of the silica surface, or alternatively, through various "ceramatisation" strategies involving the use of other metal oxide materials or the cladding of the silica surface with yttrium, zirconium, aluminium or other alkaline earth salts [8,9]. Determination of the isothermal adsorption behaviour of proteins with these and other adsorbents represents an essential aspect both for the evaluation of existing silica-based adsorbents as well as new types of ceramic-based adsorbents for their suitability in large-scale purification applications, and as an avenue to gain improved knowledge about the behaviour of proteins at solid–liquid interfaces in general.

Although the effect of changes in ionic strength and temperature can, from first principles, be anticipated to be profound, few studies have generated detailed experimental data delineating in quantitative terms the magnitude of the trends mediated by these parameters with proteins interacting with adsorbents of different ligand types derived from silica matrices with the same, or similar, physical characteristics. This study addresses some of these issues through an examination, under equilibrium batch adsorption conditions, of the isothermal behaviour of two proteins, hen egg white lysozyme (HEWL) and human serum albumin (HSA), with a range of adsorbents of different ligand selectivities, based on the use of similar silica support materials but operated under different conditions of ionic strength and temperature. Based on the outcome of these investigations, several general conclusions have been drawn with regard to the effect of the particle pore and particle size, the ligand type and density, the ionic strength and the temperature on the adsorption behaviour of these proteins with coulombic, immobilised metal ion affinity and immobilised dye affinity chromatographic adsorbents.

2. Experimental

2.1.1. Proteins

Lyophilised and dialysed HEWL (E.C. 3.2.1.17) was purchased from Sigma (Sydney, Australia). HSA [as a 20% (w/v) solution] was generously provided by CSL (Parkville, Australia). Both proteins were further purified (to >99.5% purity) and characterised using our previously described methods [1,18].

2.1.2. Chromatographic support materials

The porous silica support materials used in these investigations included LiChroprep DIOL (25–40 and 40–63 μm) and Fractosil 1000 (63–100 μm) and were obtained from E. Merck (Darmstadt, Germany).

2.1.3. Buffers

For the dye-affinity batch adsorption experiments, 50 m*M* Tris–HCl (Sigma), pH 7.0, was used as the equilibrium binding buffer. Phosphate-buffered saline (PBS), pH 7.0, prepared from 0.5 *M* sodium chloride and 0.02 *M* sodium dihydrogenorthophosphate, was used as the equilibrium binding buffer for the immobilised metal affinity adsorption (IMAC) experiments. Both salts were purchased from Merck Australia (Kilsyth, Australia). For the ion-exchange adsorption experiments, the equilibrium binding buffer consisted of 0.02 *M* sodium acetate, pH 5.2, prepared by mixing glacial acetic acid (Merck Australia) with distilled water and adjusting the pH with 5 *M* NaOH. In the dye-affinity batch adsorption experiments, the elution buffer consisted of the equilibrium binding buffer containing 0.2 *M* sodium chloride or when the elution proved to be difficult, 2.5 *M* potassium thiocyanate (Sigma) was used to elute the protein. PBS (pH 7.0) containing 50 m*M* imidazole was used as the eluting buffer for the IMAC batch adsorption experiments. The equilibrium binding buffer (0.02 *M* sodium acetate, pH 5.2, containing 0.5 *M* NaCl) was used to elute the proteins in the ion-exchange batch adsorption experiments.

2.1.4. Batch (finite bath) experiments

For the batch experiments, the apparatus was based on the instrumental system constructed as described by Anspach et al. [10] and consisted of a Model 2238 UV spectrophotometer, a Model 2132 Microperpex peristaltic pump and a Model 2210 two-pen chart recorder, all from Pharmacia Biotech (Uppsala, Sweden). Uniform temperature was ensured by the use of a recycling thermostatted bath (Model 2219 Multitemp 11), also purchased from Pharmacia Biotech.

2.1.5. Preparation of the proteins

All the protein solutions used were prepared on the same day of the individual experiments. HEWL, in powdered form, was dissolved in the required amount of the various equilibration binding buffers to make solutions of the appropriate final protein concentrations. The stock solution of HSA (20%, w/v) was divided into 1 ml aliquots and kept frozen at −20°C. When experiments were performed using HSA as the model protein, each aliquot was diluted with the various equilibration binding buffers to make up solutions of the appropriate protein concentration. The extinction coefficient of the HSA solutions was measured spectrophotometrically and calibrated against other protein standards with an A_{280} found to be equal to 0.583 for a HSA protein solution of 1 mg/ml.

2.1.6. Preparation of activated silicas for dye affinity adsorption investigations

LiChroprep DIOL or Fractosil 1000 (20 g) were suspended in 200 ml of water and adjusted to pH 3.5 by the addition of 0.01 *M* HNO_3. After rechecking the pH of the suspension, an equimolar quantity of 3-mercaptopropyltriethoxysilane (MPS) from ECA (Steinheim, Germany) was added to the silica suspension. The amount of silane added was based on the specific surface area of the total amount of silica present and an assumed content of 8 μmol of hydroxyl groups per m^2 of surface area of the corresponding silica. In the case of LiChroprep DIOL, as the surface area (500 $m^2\ g^{-1}$) was large, the amount of silane added was reduced by a factor of ten. The silica–MPS mixture was heated to 363 K for 3 h in a waterbath, with continuous shaking. After the heating process, the derivatised silica suspension was transferred to a buchner funnel, where it was extensively washed with water. After the aqueous washing was completed, the MPS-activated silica was washed with acetone, toluene and

chloroform, all purchased from Merck Australia. After reconstitution under aqueous conditions, the MPS-activated silica was stored in 0.01 *M* NaN_3 (Merck Australia) until used.

2.1.7. Preparation of activated silica for IMAC adsorption experiments

Iminodiacetic acid (IDA; 1 g), purchased from Sigma, and NaOH (1.530 g) were dissolved in 18 ml of water at 273 K and the solution was cooled in an ice-bath. 3-Glycidoxypropyltrimethoxysilane (Glymo; 1.776 g; Fluka, Castle Hill, Australia) was then added dropwise, after which, the flask was sealed. The reaction was allowed to proceed until the temperature inside the flask reached room temperature (ca. 296 K). The reaction mixture was then heated overnight at 363 K in a waterbath, with shaking. Five times the amount of Glymo–silane (8.80 g) was then added, to achieve a theoretical surface coverage of 20 μmol/m^2, and the pH was adjusted to pH 3 by the addition of 10 m*M* HNO_3. Moist silica (20 g) was then added and the suspension was heated at 363 K for 3 h. The suspension was then washed with 100 ml each of toluene, 2-propanol and water, to remove the unbound silane, and the IDA–silica was recovered by filtration.

2.1.8. Preparation of poly(succinimido)-modified silicas for ion-exchange adsorption experiments

The surface-modified polyaspartic acid immobilised onto glycidoxypropyl-modified silica for ion-exchange adsorption experiments was prepared by the method proposed by Alpert [11], but with slight modifications. Briefly, L,D-aspartic acid (50 g) was placed in a round-bottomed flask and heated at 180°C for 3 h. The dehydrated powder was dissolved with heating in 150 ml of dimethylformamide (DMF). The DMF solution was then mixed with four volumes of water and the precipitated poly(succinimide) was recovered by centrifugation. The poly(succinimide) was coupled to aminopropyl–Fractosil 1000 using a 1:1 mass ratio of the silica to the poly(succinimide) in DMF, essentially as described by Alpert [11], and then it was converted to the poly(aspartic acid)-modified Fractosil 1000 by gentle hydrolysis of the modified silica (5 g) in aqueous DMF (25 ml, 1:1) containing triethylamine (1 ml) and β-alanine (1 g) for 24 h at room temperature. The poly(aspartic acid)-modified Fractosil 1000 was recovered by filtration and washed with water, 0.05 *M* HCl, water and finally acetone, and was stored as a dry powder under nitrogen.

2.1.9. Immobilisation of Cibacron Blue F3G-A to the activated silica

The MPS-modified Fractosil was suspended in 100 m*M* Na_2CO_3–0.5 *M* NaCl, pH 8.0, containing Cibacron Blue F3GA (15 mg), purchased from Serva (Heidelberg, Germany), and the immobilisation was carried out according to the procedure described by Small et al. [12] for the modification of agarose. The reaction mixture was warmed to 363 K in a water-bath for 12 h with the silica suspension continuously shaking. The immobilised Cibacron Blue–silica was washed with 50 m*M* Tris–HCl, pH 7.8, and then washed and recentrifuged (1000 *g*) a further five times in the reaction buffer until the supernatant was colourless. The amount of dye added was calculated on the basis of the surface area of the corresponding silica and an assumed amount of 8 μmol of hydroxyl groups per m^2. In analogous experiments, the amount of dye added was reduced by a factor of ten when LiChroprep DIOL was used.

2.1.10. Equilibration of IDA–silica with Cu(II) ions

The chelating IDA–silica was washed with several volumes of Milli-Q water, after which, 50 m*M* $CuSO_4$ (Merck Australia) was added. The unbound metal ions were removed with 100 m*M* sodium acetate–1 *M* sodium chloride, pH 4.0. Finally, the IDA–Cu(II)–silica gel was equilibrated with 20 m*M* sodium phosphate containing 0.5 *M* sodium chloride, pH 7.0.

2.1.11. Procedures for the batch adsorption experiments

A stock solution of the protein (5 mg/ml) was prepared in the appropriate equilibrium binding buffer, from which different protein concentrations were made up to a final volume of 5 ml in plastic vials. The degassed adsorbents (0.5 g) were added to the protein solution and the mixture was gently agitated overnight by means of a spinning wheel incubator at 298 K (or under other controlled temperature conditions), after which the vials were

centrifuged at 5000 *g* for 10 min at the same temperature.

After centrifugation, the supernatant was carefully removed from each plastic vial and stored in a new vial. An aliquot (2 ml) of the same equilibrium binding buffer solutions, 50 m*M* Tris–HCl, pH 7.0, for the dye affinity experiments; 20 m*M* PBS, pH 7.0, for the immobilised metal affinity experiments and 20 m*M* sodium acetate buffer, pH 5.2, for the ion-exchange experiments, pre-equilibrated to the same temperature as used for the adsorption step, was then added to the pellet and after <30 s the mixture was centrifuged for 15 min at the same temperature. The supernatant was carefully removed and added to the previous recovered supernatant, making a final volume of 7 ml. Samples (1 ml) of the combined supernatants were pipetted into a quartz cuvette and the optical density was measured at 280 nm using the Pharmacia 2238 UV spectrophotometer. The amount of protein adsorbed onto each adsorbent was determined from the difference between the protein concentration initially added to the vial and that found in the supernatant afterwards. In this parallel fashion, batch adsorption experiments were performed at four different temperatures (4, 15, 25 and 37°C), with the buffers and adsorbent kept for 24 h at the selected temperature before being used. All experimental data represent the average of triplicate measurements.

3. Results and discussion

3.1. Theoretical background to equilibrium adsorption in finite bath systems

Although the Langmuir isothermal model [13] was initially conceived to describe the adsorption of gases to glass and mica surfaces, where equilibrium is quickly established, this adsorption model has also found relatively wide application as a convenient representation of the simplest cases of the surface interaction of a protein (P) with a ligand (L), immobilised onto a porous support material. Various practical examples of the use of the Langmuir isothermal model can be found in the scientific literature and include the adsorption of lysozyme onto Blue–Sepharose [14], the adsorption of HSA, lysozyme and alcohol dehydrogenase to Cibacron Blue F3G-A immobilised onto Sepharose CL-6B, Sepharose 4B, Gelatine GC700, Fractogel HW 55F, HW 65F, HW 75F, Spherosil XOBO30 or Nucleosil [15] and the adsorption of BSA onto cross-linked chitosan [16].

When the protein is relatively small and the immobilised ligand is readily accessible, the overall dynamics of the adsorption can be fast and the assumption of local equilibrium may be valid. The Langmuir model represents a simplified case of protein adsorption, since this model assumes (a) reversible adsorption, (b) no change in the properties of the adsorbed molecules, (c) no lateral interaction between adsorbed molecules, (d) one adsorption site per molecule and (e) that all adsorption sites have the same affinity for the protein. Under such assumptions, the binding of a protein onto an immobilised ligand can be represented by the following equilibrium:

$$P + L \underset{k_2}{\overset{k_1}{\rightleftharpoons}} PL \tag{1}$$

where the forward (k_1) and reversed (k_2) interaction rates take into account the mass transfer resistances, which include the protein movement from the bulk mobile phase to the adsorbent surface layer, the protein transfer across a stagnant film layer surrounding the adsorbent particles, the protein diffusion into the pores of the particles and the interaction and adsorption of protein to the solid phase (Fig. 1). Eq. (1) can be expressed in the form of a rate equation with a second-order forward and first-order reverse kinetics, namely:

$$\frac{dq}{dt} = k_1 C^*(q_m - q^*) - k_2 q \tag{2}$$

where C^* is the concentration of the protein in the mobile phase (bulk solution), q^* is the amount of protein adsorbed onto the matrix and q_m is the maximum capacity of the matrix. At equilibrium (denoted by the asterisk), the rate of forward interaction becomes equal to the rate of reverse interaction, dq/dt becomes zero and Eq. (2) can be converted to:

$$q^* = \frac{q_m C^*}{K_d + C^*} \tag{3}$$

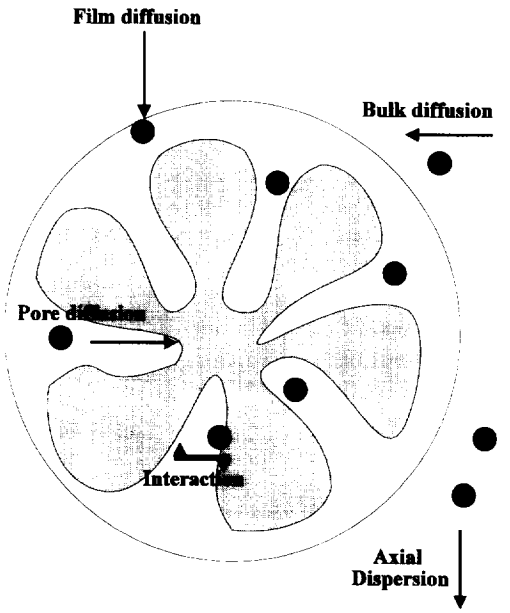

Fig. 1. Schematic representation of the dynamic adsorption and mass transfer effects of a protein molecule with a porous adsorbent particle.

where K_d represents the dissociation constant.

Over the past decade, various investigations related to the adsorption of proteins to chemically modified surfaces have shown that these assumptions, implicit to the Langmuirean model for bimolecular interactions, may not be fulfilled. The protein may undergo conformational changes or other types of secondary equilibrium upon binding or in solution, leading to deviations from the Langmuir isotherm. The adsorbents are also likely to possess a number of different adsorption sites, arising from imperfect manufacturing. Recognition of this heterogeneity has led to the derivation of numerous, more complex, isothermal expressions, including the Freundlich, multicomponent Langmuir, Freundlich–Langmuir, Redlich–Peterson, Fowler, Javanovic and S-shaped isotherms [17–22].

The Freundlich equation [17] is the empirical relationship whereby it is assumed that the adsorption energy of a protein binding to a site on an adsorbent depends on whether or not the adjacent sites are already occupied. This empirical expression takes the form:

$$q^* = \kappa(C^*)^{\eta} \tag{4}$$

where κ and η are empirical coefficients. The adsorption of novobiocin onto the anion-exchange resin, Dowex 21 K [23], and the adsorption of cephalosporin C onto the hydrophobic resin, Amberlite XAD [24], have been successfully characterised in terms of the Freundlich model. One limitation of the Freundlich model is that the amount of adsorbed solute increases indefinitely with the concentration of solute in the solution. This limitation can be overcome by combining the Freundlich model with the Langmuir model, which can be represented by Eq. (5):

$$q^* = \frac{q_m(C^*)^{\eta}}{K_d + (C^*)^{\eta}} \tag{5}$$

Although the Freundlich–Langmuir equation can be used to model adsorption co-operativity [25], the combination of the Langmuir and the Freundlich expressions is more often applied on a strictly empirical basic, since the extra parameter (η) ensures an improved correlation with the equilibrium data, compared to the simple Langmuir isotherm [13]. For example, in our previous studies related to the adsorption of HEWL to IMAC adsorbents with high ionic strength buffers (i.e. $I>2.0$), it was observed that adsorption cooperativity is characteristic of isodesmic, indefinite interactions involving protein–ligand and protein–protein self-association. In this investigation of the adsorption of HEWL and HSA to different adsorbents, comparative assessments were made in terms of the degree of fit of the experimental data to the Langmuir and Freudlich models for the adsorption of a protein to an immobilised ligand. In a subsequent paper, evaluation of the adsorption behaviour of several of these globular proteins, in terms of the multicomponent Langmuir, Freundlich–Langmuir, Redlich–Peterson, Fowler, Javanovic and S-shaped isotherms, will be described.

3.2. General considerations

From the experimental data obtained from the batch adsorption experiments with the different adsorbents under different ionic strength and temperature conditions, the adsorption isotherms reflecting the equilibrium capacity of the adsorbent, at a particular concentration of protein in solution, were

constructed. The maximum capacity (q_m) and the dissociation constant (K_d) were extracted from the corresponding semi-reciprocal plots (C^*/q^* versus C^*). The semi-reciprocal plot was chosen instead of the double reciprocal plot (C^*/q^* vs. C) on the basis of least squares regression analyses of the experimental data. Moreover, the adsorption values for the proteins at higher concentrations contribute more significantly to the regression analysis of the semi-reciprocal plot [27]. The characteristics of the adsorption process were also investigated using Scatchard plot analysis (q^*/C^* versus q^*). When the Scatchard plot showed a deviation from linearity, greater emphasis was placed on the analysis of the adsorption data in terms of the Freundlich model, in order to construct the adsorption isotherms of the protein(s) at particular concentration(s) in solutions of different ionic strength or temperature.

Fig. 2 shows the adsorption isotherm of HEWL with immobilised Cibacron Blue F3G-A–LiChroprep DIOL under different salt concentrations, whilst Fig. 3 presents the adsorption characteristics assessed from the Scatchard plot. In the absence of NaCl, deviation from linearity in the plot of q^*/C^* versus q^* was observed, indicating the presence of multimodal interaction and non-Langmuirean behaviour. At least three types of interactions can occur during the adsorption process, namely, (i) specific binding involving biomimetic interactions between the dye and the protein, (ii) non-specific binding between the protein and other classes of binding sites on the adsorbent and (iii) protein–protein interaction involving inter alia changes in protein conformation. The corresponding semi-reciprocal transformations (Fig. 4) of the equilibrium binding data for HEWL and immobilised Cibacron Blue F3G-A–LiChroprep DIOL in the presence of 0.05 M NaCl gave rise to a linear plot, indicating that the Langmuir model could be applied in this case. However, in the range of 0.1–0.2 M NaCl, divergence from the linear semi-reciprocal fit was again evident, consistent with the participation of secondary equilibrium effects in the adsorption process.

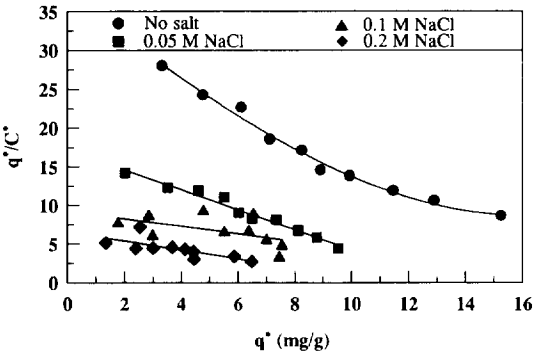

Fig. 3. Scatchard plot of the experimental data for the adsorption of HEWL at different salt concentrations to Cibacron Blue F3G-A immobilised onto LiChroprep DIOL.

In order to ascertain the effect of protein size on the adsorption process with this adsorbent, identical experiments were carried out using HSA and the corresponding adsorption isotherms generated for HSA binding to Cibacron Blue F3G-A immobilised onto LiChroprep DIOL under different NaCl con-

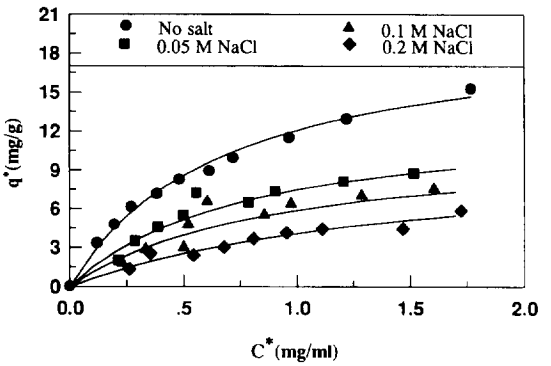

Fig. 2. Adsorption isotherms for the batch equilibrium binding of HEWL at different salt concentrations to Cibacron Blue F3G-A immobilised onto LiChroprep DIOL.

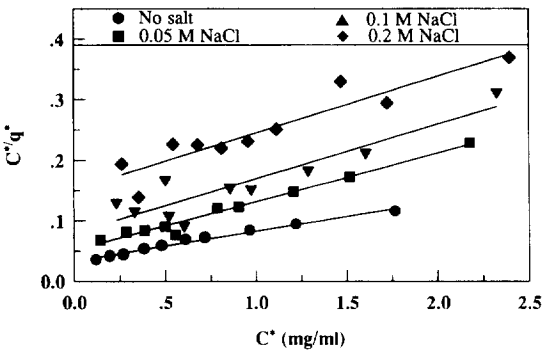

Fig. 4. Semi-reciprocal plot of the experimental data for the adsorption of HEWL at different salt concentrations to Cibacron Blue F3G-A immobilised onto LiChroprep DIOL.

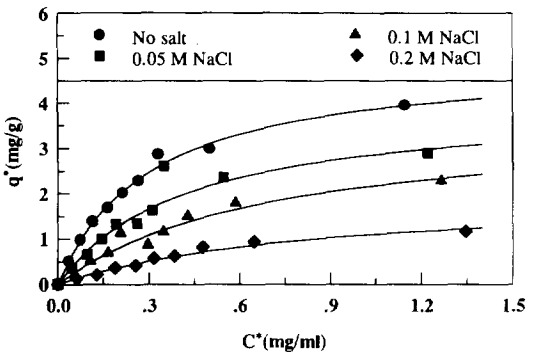

Fig. 5. Adsorption isotherms for the batch equilibrium binding of HSA at different salt concentration to Cibacron Blue F3G-A immobilised onto LiChroprep DIOL.

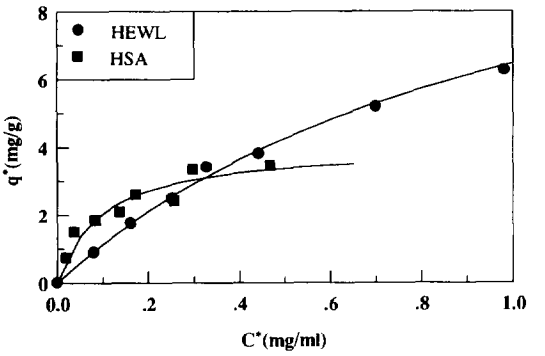

Fig. 6. Comparison of the adsorption isotherms for the binding of HEWL and HSA to Cibacron Blue F3G-A immobilised onto Fractosil 1000.

centrations (Fig. 5). The resulting Scatchard plot analysis indicated that the adsorption of HSA onto immobilised Cibacron Blue F3G-A could also be satisfactorily modelled using the Langmuir model. Consistent with the difference in the molecular diameter of HSA (ca. 83.5 Å using the formula derived by Travers and Church [28]) compared to HEWL (which is about 27.3 Å) and the distribution of surface-accessible amino acid residues believed to be involved in the interaction of the Cibacron Blue F3G-A triazine dye, at the same ionic strength, the q^* value for HSA was approximately three-fold lower than the corresponding value for HEWL.

To compare the adsorption behaviours of these two proteins with the same ligand immobilised onto support materials of different porosities, the equilibrium adsorption curves for the binding of HEWL and HSA to Cibacron Blue F3G-A immobilised onto LiChroprep DIOL and Fractosil 1000, are shown in Figs. 2, 5 and 6. As evident from these data, the adsorption isotherm of HSA–Cibacron Blue F3G-A–Fractosil 1000 was steeper than the corresponding isotherm for HEWL–Cibacron Blue F3G-A–Fractosil 1000, indicating a greater affinity of HSA for Cibacron Blue F3G-A when immobilised to Fractosil 1000. A similar effect was not as apparent when Cibacron Blue F3G-A was immobilised onto LiChroprep DIOL. With the latter adsorbent, the binding of HEWL could not be as adequately represented by the Langmuir model, but rather followed more closely the Freundlich model (Fig. 7). As noted above, possible reasons for this difference may be associated with the presence of more than one kind of binding site involved in the adsorption of lysozyme to Cibacron Blue F3G-A immobilised onto LiChroprep DIOL, and indicative of more complex binding phenomena than can be explained in terms of the independent and univalent binding site Langmuirean model [13]. Analogous conclusions have been reached in studies on the binding of HEWL to various IMAC adsorbents, where processes characteristic of similar isodesmic self-association have been observed [26].

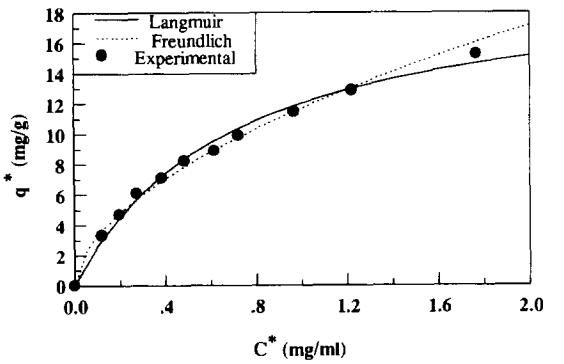

Fig. 7. Comparison of the experimental and the predicted adsorption isotherms derived from the Langmuir and Freundlich equations, Eqs. (3) and (4), respectively, with the batch equilibrium binding data of HEWL to Cibacron Blue F3G-A immobilised onto LiChroprep DIOL.

3.3. Effect of temperature on the adsorption isotherms

In a similar manner to that employed for the experiments involving a change in ionic strength, from the experimental equilibrium binding data generated at different temperatures, the corresponding adsorption isotherms were constructed and the equilibrium parameters (q_m and K_d) were determined from the corresponding semi-reciprocal plots. The equilibrium association constant, (K_a) extracted from the semi-reciprocal plot was then employed for Van't Hoff plot analysis of log K_a versus the reciprocal of the temperature (in K). From the Van't Hoff plot, the apparent thermodynamic parameters (ΔG_{assoc}, ΔH_{assoc} and ΔS_{assoc}) were then extracted. It should be noted that the thermodynamic parameters extracted are apparent values, since the phase ratio (R_v), i.e. the ratio of the volume of stationary to mobile phase in the finite bath is not specified at the different temperatures, however, for the purpose of these analyses, it was assumed to be constant. The value of the apparent change in enthalpy (ΔH_{assoc}) during the binding process was determined from the gradient of the plots and can be equated inter alia with the extent of hydrogen bond formation or breakage. The corresponding values of the apparent change in free energy (ΔG_{assoc}) and the apparent change in entropy (ΔS_{assoc}) were determined from the relationships $\Delta G_{assoc} = -RT \ln K_a$ and $\Delta G_{assoc} = \Delta H_{assoc} - T\Delta S_{assoc}$, where R is the gas constant.

3.3.1. Adsorption isotherms for HEWL and HSA binding to Cibacron Blue F3G-A immobilised onto Fractosil 1000 under different temperature conditions

The adsorption isotherms for the binding of HEWL and HSA to Cibacron Blue F3G-A immobilised onto Fractosil 1000 at different temperatures are shown in Figs. 8 and 9, respectively. Equilibration buffer conditions were selected which had previously been shown to favour a single component adsorption process consistent with Langmuirean behaviour. The adsorption isotherms derived from the semi-reciprocal plots were steeper at higher temperature, indicating interactions of greater affinity between the protein and the adsorbent. For all of the temperature conditions, the Scatchard plots were linear, indicating that the mode of interaction as the temperature was increased with these two proteins and the immobilised dye was consistent with Langmuirean behaviour.

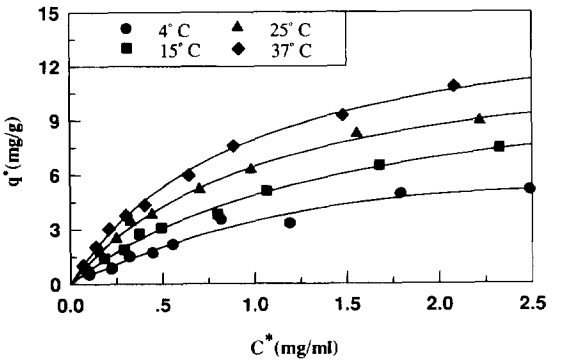

Fig. 8. Adsorption isotherms for the batch equilibrium binding of HEWL at different temperatures to Cibacron Blue F3G-A immobilised onto Fractosil 1000.

3.3.2. Adsorption isotherms for HEWL and HSA binding to IDA–Cu^{2+} immobilised onto Fractosil 1000 under different temperature conditions

The adsorption isotherms for the binding of HEWL and HSA onto immobilised IDA–Cu^{2+}, derived from the semi-reciprocal plots, are represented in Figs. 10 and 11, respectively. The Scatchard plot showed deviation from linearity, indicating that the Langmuir model could only be applied

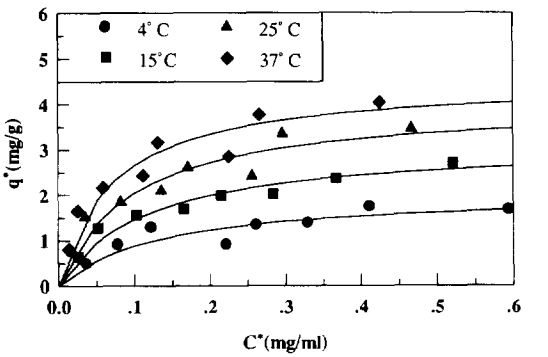

Fig. 9. Adsorption isotherms for the batch equilibrium binding of HSA at different temperatures to Cibacron Blue F3G-A immobilised onto Fractosil 1000.

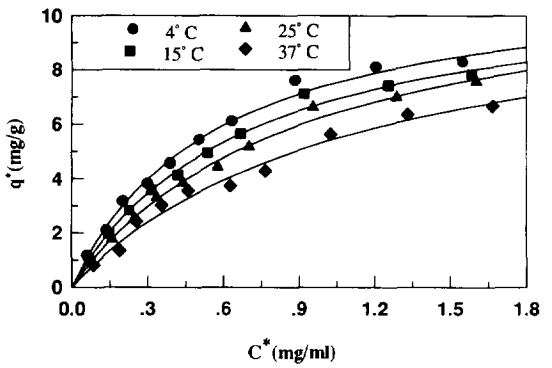

Fig. 10. Adsorption isotherms for the batch equilibrium binding of HEWL at different temperatures to IDA–Cu^{2+} immobilised onto Fractosil 1000.

over a relatively small range of conditions for the adsorption process with these proteins and the immobilised IDA–Cu^{2+}. The equilibrium binding curves were steeper at lower temperature, indicating a higher affinity between the IMAC ligand and both proteins at lower temperatures. As is also evident from extrapolation of the results, all of the plots derived from the Scatchard analysis converged to one point on the x-axis (q^*), indicating that no change in q_{max} occurred when the temperature was increased from 4 to 37°C. This outcome was not as evident directly from the plot of C^* versus q^* in the range of concentration studied. Moreover, this convergence of the experimental data obtained at different temperatures to a common point on the q^*-axis indicates that the molecular forces that contribute to the interaction between the protein and the immobilised IDA–Cu^{2+} are not hydrophobic in character. At higher temperature, both test proteins would be expected to progressively commence to unfold and to expose buried hydrophobic amino acid residues. If the interaction between the protein and the immobilised ligand involved a significant hydrophobic contribution, the contact surface between the protein and the immobilised ligand should increase at higher temperatures, resulting in an increase in the affinity of both proteins for the adsorbent at higher temperature. In fact, the opposite is observed experimentally, with the convergence of the data points at the different temperatures being consistent with the formation of coordination bonds between the protein and the immobilised metal ion [29–31].

3.3.3. Adsorption isotherms for HEWL binding to polyaspartic acid immobilised onto Fractosil 1000 under different temperature conditions

Fig. 12 shows the adsorption isotherms for the binding of HEWL to polyaspartic acid immobilised onto Fractosil 1000. The equilibrium binding curve derived from the semi-reciprocal plot showed that, at low temperature, significant deviation of the experimental data at high protein concentrations was observed from the predicted Langmuir model isotherm. This observation was confirmed by the Scatchard plot analysis, where deviation from linear dependencies was observed (Fig. 13). Since, at low temperatures, the adsorption of HEWL onto immobilised polyaspartic acid cannot be described in terms of the Langmuir model, the ability of the

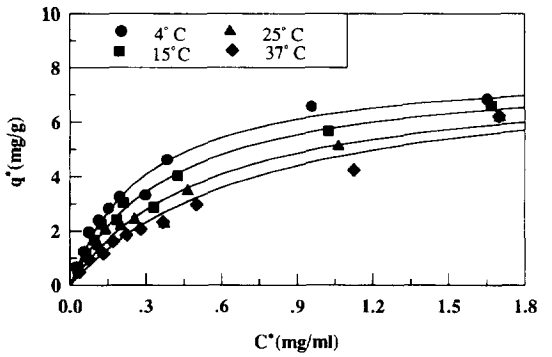

Fig. 11. Adsorption isotherms for the batch equilibrium binding of HSA at different temperatures to IDA–Cu^{2+} immobilised onto Fractosil 1000.

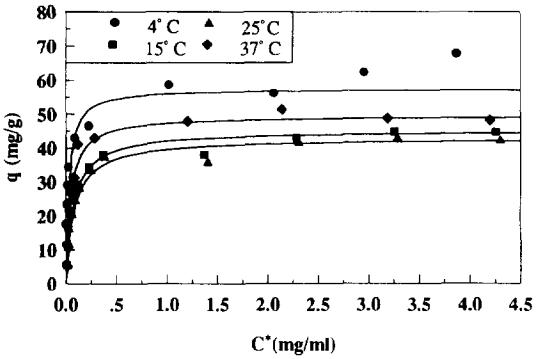

Fig. 12. Adsorption isotherms for the batch equilibrium binding of HEWL at different temperatures to polyaspartic acid immobilised onto Fractosil 1000.

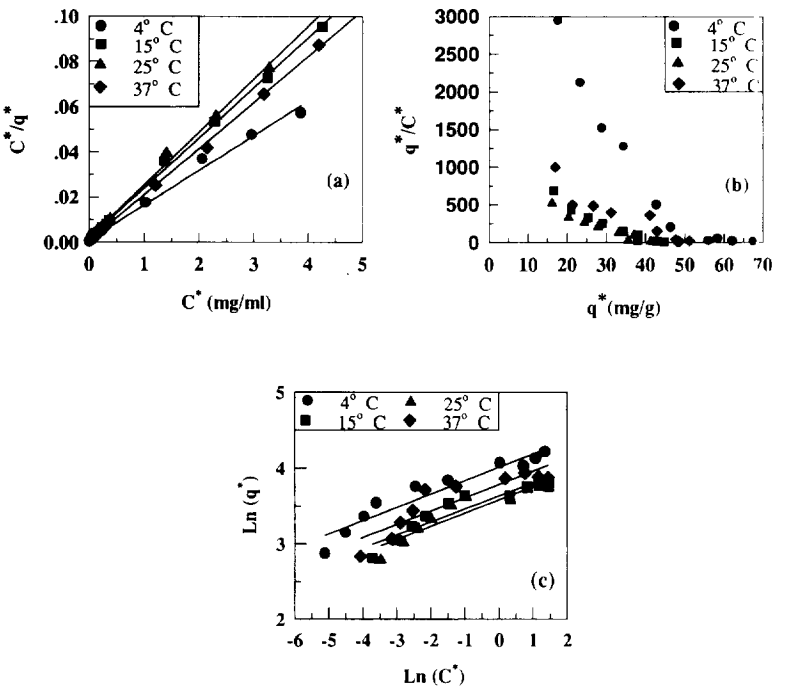

Fig. 13. (a) Semi-reciprocal plot, (b) Scatchard plot and (c) log–log plot of the experimental data for the adsorption of HEWL at different temperatures to polyaspartic acid immobilised onto Fractosil 1000.

Freundlich model to fit the experimental data was consequently examined. The equilibrium binding resulting from the Freundlich and the Langmuir models are shown in Fig. 14. In Fig. 14a, both models fitted the lower portion of the equilibrium binding data obtained for the 4°C investigation reasonably well, i.e. $\Sigma_{\text{variances}}\sigma^2$ resulted in small values. However, at higher protein concentrations, the Freundlich model more closely approximated the experimental data. In contrast, at 15°C, the adsorption plot more closely approximated the single component Langmuirean isotherm. However, as evident from Fig. 13b, the Scatchard plots of the experimental data obtained at temperatures greater than 15°C showed significant deviation from linearity, suggesting that other types of isothermal behaviour were occurring.

3.4. Effect of changes in ionic strength, pore size and particle diameter on the equilibration binding parameters

Equilibrium binding parameters were derived from a single-component or a two-component Langmuir or Freundlich-type analysis by regression analysis of the experimental data for HEWL and HSA with the different adsorbents. In the case of Langmuir-type fit of the experimental data, the semi-reciprocal plot of C^*/q^* versus C^* was employed to generate the intercept of K_d/q_m and the slope of $1/q_m$. In the case of the Freundlich-type fit of the experimental data, the plot of log C^* versus log q^* was employed to generate the intercept value of log κ and the slope of η.

As evident from the maximum capacity (q_{max}) and the dissociation constant (K_d) data for adsorption of HEWL and HSA to the immobilised Cibacron Blue F3G-A LiChroprep DIOL adsorbents, shown in Tables 1 and 2, the maximum binding capacity of both proteins was reduced by the increasing presence of salt. When HEWL was equilibrated in 0.05 *M* Tris–HCl–0.2 *M* NaCl with the dye affinity matrix prepared from the LiChroprep Diol (40–63 μm), the q_{max} for the protein was reduced by 32% compared to the NaCl-free condition. The presence of the same salt concentration in the equilibration buffer similarly

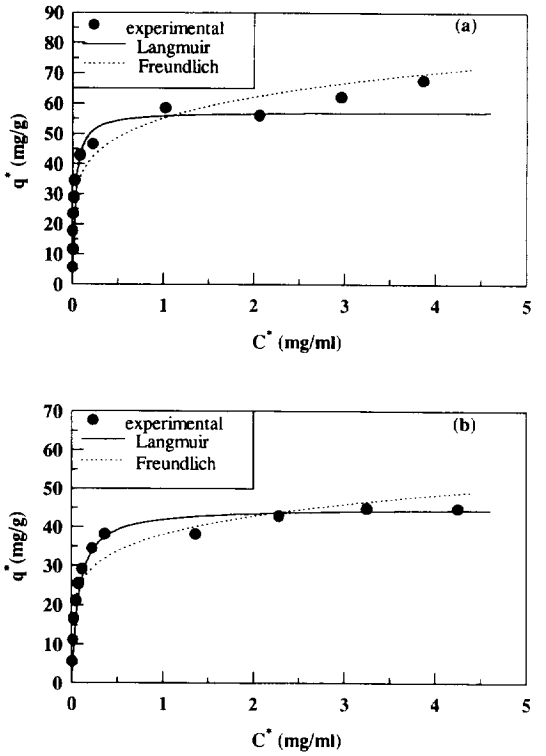

Fig. 14. Comparison of the experimental and the predicted adsorption isotherms derived from the Langmuir and Freundlich equations, Eqs. (3) and (4), respectively, with the batch equilibrium binding data of HEWL at (a) 4°C and (b) 15°C, to polyaspartic acid immobilised onto Fractosil 1000.

reduced the q_{max} value for HSA by 60%. Similar results have been obtained by Boyer and Hsu [32] in their study of the adsorption of HSA and lysozyme onto Cibacron Blue F3G-A immobilised onto Sepharose CL-6B. The significant decrease in q_{max} for the binding of HSA onto immobilised Cibacron Blue F3G-A in the presence of an increasing concentration of NaCl confirms that the origin of forces involved during the adsorption process of HSA with this triazine dye ligand is mainly coulombic [28]. Similarly, the small decrease in q_{max} for the binding of HEWL to the immobilised dye leads to the conclusion that a mixture of electrostatic and hydrophobic forces are involved during the binding process with this protein. The combination of forces involved during the adsorption process with HEWL is not surprising, taking into account the relatively high surface hydrophobicity of this protein and the ability of triazine dyes to act as multi-functional ligands that contain both hydrophobic and charged groups [32,33]. In addition, the experimental results also confirm that the binding capacities of the immobilised Cibacron Blue F3G-A LiChroprep DIOL adsorbent for these two proteins is dependent on protein size. HEWL, which has a low molecular mass of 14 400 shows higher binding capacities than HSA (67 000) on both a mass and molar basis. On a mass basis, immobilised Cibacron Blue F3G-A binds four times more HEWL than HSA, which translates to a seven-fold factor on a molar basis.

In circumstances where the adsorption process obeys the Langmuir isotherm, the percentage of ligand utilisation representing the fraction of ligand that binds to the protein can be readily determined from the molar ratio of the maximum binding capacity to ligand concentration [34]. The results for the immobilised Cibacron Blue F3G-A LiChroprep DIOL and Fractosil 1000 adsorbents are shown in Table 3. For the larger, 40–63 μm particle LiChroprep DIOL support material, HEWL bound to 30% of the immobilised Cibacron Blue F3G-A ligands, while HSA bound to only 2.1% of the immobilised Cibacron Blue F3G-A. Since LiChroprep DIOL has an average pore size of 60 Å, HSA with a molecular diameter of 83.5 Å will be effectively excluded from the pores. Hence, the amount of immobilised dye available to HSA will be considerably smaller than that accessible to the HEWL. Steric effects and pore blockage will also contribute to the lower amount of dye accessible to both HEWL and HSA. Taking into account the relative size of the protein and dye ligands, the 2.1% ligand involvement with HSA suggests that the assumption of monovalent interaction between HSA (or HEWL) and the dye ligands is an over-simplification of the adsorption process and that multi-site attachment occurs, consistent with other observations [29] and the present observation of a higher affinity for the HSA–ligand interaction.

The effect of particle size was evident from the experiments involving Cibacron Blue F3G-A immobilised onto LiChroprep DIOL (25–40 and 40–63 μm) and Fractosil 1000 (40–63 and 63–100 μm). The results are shown in Table 4. The maximum value of the binding capacities increased with decreasing particle size, but not in proportion to the

Table 1
The q_m and K_d values derived for a single-component Langmuir equilibrium binding process obtained from the experimental data for the interaction of HEWL and HSA to Cibacron Blue F3G-A immobilised onto LiChroprep DIOL, with average particle diameters of 40–63 and 25–40 μm in the presence of different NaCl concentrations

Cibacron Blue F3G-A immobilised onto LiChroprep DIOL	q_m (mol^{-1})$\times 10^{-7}$ g^{-1}	K_d (M)$\times 10^{-5}$
LiChroprep DIOL (40–63 μm)		
HEWL (no NaCl, high affinity)[a]	11.3	3.22
HEWL (no NaCl, low affinity)[a]	17.2	9.34
HEWL (50 m*M* NaCl)	9.58	5.71
HEWL (100 m*M* NaCl)	8.05	6.57
HEWL (200 m*M* NaCl)	7.63	11.5
HSA (no salt)	0.76	0.46
HSA (50 m*M* NaCl)	0.61	0.64
HSA (100 m*M* NaCl	0.56	1.07
HSA (200 m*M* NaCl	0.31	1.36
LiChroprep DIOL (25–40 μm)		
HEWL (no NaCl, high affinity)[a]	13.1	1.63
HEWL (No NaCl, low affinity)[a]	19.0	4.76
HSA (no salt)	0.89	0.28

The experimental data were fitted to Eq. (3) according to the procedures described in Section 2.
[a]The Scatchard plots for HEWL under these conditions showed deviation from linearity in the plots of c^*/c versus c.
The q_m and K_d values were fitted to a two-component model and the corresponding high and low affinity values were determined for each component.
The curve saturated at low protein concentration was called the high affinity curve.

increase in the total surface area. A reduction in the particle size had the opposite effect on the equilibrium parameters (K_d and q_m). An increase in the maximum capacities of the adsorbent for the protein was obtained, whilst a reduction in the dissociation constant was observed (cf. Table 1). The degree of change in the association constants, however, was much greater than the degree of change in the maximum capacities. The effect was particularly pronounced with HEWL, where a 15% increase in capacity was associated with a 100% increase in the association constant when the mean particle size was reduced from 51.5 to 32.5 μm. A similar trend was observed when Fractosil 1000 was employed instead of LiChroprep DIOL (Table 4). A 26% increase in the binding capacity for HEWL was obtained compared to a 74% change in the association constant when the mean particle size of the Fractosil 1000 was reduced from 81.5 to 51.5 μm. Such variation in the values of these parameters will have profound and different effects on the performance of these adsorbents in packed-bed and fluidised-bed or expanded-bed column systems [35].

Table 2
The κ and η values derived for a single-component Freundlich equilibrium binding process obtained from the experimental data for the interaction of HEWL to Cibacron Blue F3G-A immobilised onto LiChroprep DIOL

Cibacron Blue F3G-A immobilised onto LiChroprep DIOL	κ (mol^{-1})$\times 10^{-7}$ g^{-1}	η
LiChroprep DIOL (40–63 μm)		
HEWL (no NaCl added)	8.14	0.55
HEWL (50 m*M* NaCl)	5.09	0.59
HEWL (100 m*M* NaCl)	4.02	0.62
HEWL (200 m*M* NaCl)	2.72	0.65
LiChroprep DIOL (25–40 μm)		
Lysozyme (no NaCl added)	9.56	0.64

The experimental data were fitted to Eq. (4) according to the procedures described in Section 2.

The effect of pore size differences was also examined with the immobilised Cibacron Blue F3G-A–LiChroprep DIOL (40–63 μm) and Fractosil 1000 (40–63 μm) adsorbents, respectively. The pore size of Fractosil 1000 is 1000 Å and that of LiChroprep DIOL is 60 Å. The results, shown in Table 3, indicate that the amount of protein bound to the adsorbent was independent of the pore size.

Table 3
Relationship between the ligand concentration of the Cibacron Blue F3G-A immobilised onto LiChroprep DIOL and Fractosil 1000 adsorbents and the binding capacity

Adsorbent	Amount of Cibacron Blue F3G-A dye immobilised (μmol g^{-1})	q_m for HEWL (μmol g^{-1})	Average amount of ligand surface accessible to HEWL (%)	q_m for HSA (μmol g^{-1})	Average amount of ligand surface accessible to HSA (%)
LiChroprep DIOL (25–40 μm)	3.96	1.31	33	0.09	2.3
LiChroprep DIOL (40–63 μm)	3.74	1.13	30	0.08	2.1
Fractosil 1000 (40–63 μm)	1.92	1.21	63	0.08	4.2
Fractosil 1000 (63–100 μm)	1.61	0.95	59	0.06	3.4

Since the amount of Cibacron Blue F3G-A immobilised onto LiChroprep DIOL was found to be approximately twice the amount of the same dye immobilised onto Fractosil 1000, but the amount of protein bound to Cibacron Blue F3G-A immobilised on LiChroprep DIOL and Fractosil 1000, respectively, was in the same range, it can be concluded that steric effects prevail with the LiChroprep DIOL matrix, causing a reduction in the binding capacity when the dye concentration was increased. Similar observations have been made by various other investigators with different types of porous adsorbent materials [1,8,9,27,32,36–38].

3.5. Evaluation of the temperature effects on the equilibrium parameters

3.5.1. Equilibrium adsorption behaviour of HSA and HEWL with the Cibacron Blue F3G-A immobilised onto Fractosil 1000

Both HSA and HEWL showed a greater binding capacity with the immobilised Cibacron Blue F3G-A Fractosil 1000 adsorbents at higher temperature. The maximum binding capacity was derived from the semi-reciprocal plots and the results are shown in Table 5. From 4 to 37°C, the binding capacity of Cibacron Blue F3G-A immobilised onto Fractosil 1000 for HEWL and HSA increased by 77 and 111%, respectively. The increase in binding capacity between immobilised Cibacron Blue F3G-A and HEWL at higher temperature indicates that the binding between the protein and the immobilised Cibacron Blue F3G-A is mainly hydrophobic. At 25°C, it was observed that the addition of NaCl accentuated the participation of both coulombic and hydrophobic effects in the interaction between the protein and the immobilised dye. From the above results, it is apparent that at higher temperature, the hydrophobic effects predominate.

The addition of NaCl considerably reduced the binding capacity of the immobilised Cibacron Blue F3G-A for HSA, indicating that coulombic forces are the main forces prevailing during the adsorption process with this protein. When electrostatic inter-

Table 4
Comparison between the surface area of the immobilised Cibacron Blue F3G-A–LiChroprep DIOL and –Fractosil adsorbents of different particle diameters and the capacity for the HEWL and HSA

Adsorbent	Mean particle diameter $\times 10^{-4}$ cm	% Increase in the maximum capacity[a]		% Increase in external surface area[a]
		HEWL	HSA	
LiChroprep DIOL	51.5	–	–	–
	32.5	16 (high affinity) 10.5 (low affinity)	17.5	58.6
Fractosil 1000	81.5	–	–	–
	51.5	26.8	32.8	58.3

[a]The percentage values were calculated relative to the value of the 51.5 μm LiChroprep DIOL and 81.5 μm Fractosil 1000 particles, respectively.

Table 5
The q_m and K_d values derived for a single-component Langmuir equilibrium binding process obtained from the isothermal data for the interaction of HEWL and HSA to Cibacron Blue F3G-A immobilised onto Fractosil 1000, with average particle diameters of 40–63 and 63–100 μm at different temperatures

Cibacron Blue F3G-A immobilised onto Fractosil 1000	q_m (mol^{-1})×10^{-7} g^{-1}	K_d (M)×10^{-5}
Fractosil 1000 (63–100 μm)		
HEWL (4°C)	6.63	13.1
HEWL (15°C)	8.61	10.4
HEWL (25°C)	9.54	7.65
HEWL (37°C)	11.1	6.85
HSA (4°C)	0.31	0.023
HSA (15°C)	0.48	0.017
HSA (25°C)	0.61	0.015
HSA (37°C)	0.69	0.011
Fractosil 1000 (40–63 μm)		
HEWL (25°C)	12.1	4.32
HSA (25°C)	0.81	0.013

The experimental data were fitted to Eq. (3) according to the procedures described in Section 2.

action is involved between an adsorbent and an adsorbate, an increase in temperature should cause a decrease in the binding capacity. From our results, the opposite trend was observed. However, it can be noted that if the interaction between the protein and the immobilised dye is exothermic (ΔH is negative), an increase in temperature would favour the binding process, as long as the protein is not denatured [38].

3.5.2. Equilibrium adsorption behaviour of HSA and HEWL with the IDA–Cu^{2+} immobilised onto Fractosil 1000

For all of the temperature conditions studied with the selected equilibration buffer, Scatchard plot analysis of the experimental data indicated a linear dependency of q^*/c^* versus c^*, indicating that the Langmuir model could be used to describe the mode of interaction between the respective proteins and immobilised IDA–Cu^{2+}–Fractosil 1000. The values of q_m and K_d, derived from the semi-reciprocal plots, are shown in Table 6. Contrary to the limited change in the binding capacity for the respective proteins with the immobilised IDA–Cu^{2+} adsorbent, the affinity of IDA–Cu^{2+}–Fractosil 1000 for both proteins was considerably reduced at higher temperature. At 0°C, for example, the K_d of HEWL was 42.2 μM. At 15°C, the K_d was increased to 49.6 μM and at 37°C, the K_d was further increased to 80.9 μM. A

Table 6
The q_m and K_d values derived for a single-component Langmuir equilibrium binding process obtained from the isothermal data for the interaction of HEWL and HSA to IDA–Cu^{2+} immobilised onto Fractosil 1000, with an average particle diameter of 63–100 μm at different temperatures

IDA–Cu^{2+} immobilised onto Fractosil 1000	q_m (mol^{-1})×10^{-7} g^{-1}	K_d (M)×10^{-5}
HEWL (4°C)	8.44	4.22
HEWL (15°C)	8.22	4.96
HEWL(25°C)	8.58	6.50
HEWL (37°C)	8.16	8.09
HSA (4°C)	1.23	0.46
HSA (15°C)	1.21	0.60
HSA (25°C)	1.19	0.83
HSA (37°C)	1.22	1.13

The experimental data were fitted to Eq. (3) according to the procedures described in Section 2.

greater increase in the dissociation constant was observed in the case of HSA. As a consequence, the influence of steric (Van der Waals) and hydrogen-bonding interactions per se can be excluded as contributing to the interaction between either proteins and the immobilised IDA–Cu^{2+}–Fractosil 1000. Rather, an entropy-driven process incorporating both coordination bonding and hydrophobic effects, which will generally increase with increasing temperature ($\Delta G \propto -T\Delta S$) within a certain range [26,39], seems to occur. The reduction in the value of the association constant can be attributed to conformational changes in the protein, resulting in variation in the (time averaged) accessibility of the histidinyl residues of the protein to the ligand. HEWL has only one histidinyl residue located on the surface [40], at His 15, compared to three histidinyl residues located on the surface of HSA [41]. Greater accessibility to the histidinyl residues on the surface of HSA compared to HEWL is indicated from the higher association constant of HSA for the immobilised IDA–Cu^{2+}–Fractosil 1000 (Table 6). The decrease in affinity at higher temperatures could also be due to a reduction in the degree of ionisation of the amino acid residues associated with the binding site, thus causing the pK_a and thus the lone pair electron donor properties of the solvent-exposed histidinyl residues to change [39].

3.5.3. Equilibrium adsorption behaviour of HEWL with the polyaspartic acid immobilised onto Fractosil 1000

The q_{max} and K_d were determined from the semi-reciprocal plot for the equilibrium binding of HEWL to polyaspartic acid immobilised onto Fractosil 1000 and the results are shown in Table 7. A decrease in binding capacity at higher temperature followed by a small increase was observed for the adsorption of HEWL onto polyaspartic acid–Fractosil 1000 at different temperatures. The affinity of this cation-exchanger for HEWL followed the same trend. The change in affinity and binding capacity of the adsorbent for the protein could be due to the interplay of both hydrophobic and electrostatic forces. At low temperatures, the electrostatic effect will prevail, whilst the hydrophobic effect becomes more significant at higher temperatures. Thus, with polyaspartic acid immobilised onto Fractosil 1000, the HEWL may initially be captured electrostatically, but once brought into close proximity to the polymer layer of the stationary phase, secondary hydrophobic interactions can occur [42].

Scatchard plot analysis showed a deviation from linearity (Fig. 13), indicating that the interaction between HEWL and the immobilised polyaspartic acid Fractosil 1000 cation-exchanger cannot be represented in terms of a simple single component Langmuir model. As a result, the adsorption of HEWL onto immobilised polyaspartic acid Fractosil 1000 was examined in terms of the Freundlich model (Fig. 14). Variations in the κ-value were observed with an increase in temperature, while the other parameter, η, was unaffected by any change in temperature. The κ-values obtained from the Freundlich model were within a similar range as the q_m values obtained from the Langmuir model at different temperatures (Table 7).

3.6. Evaluation of the thermodynamic parameters

The dependency of the equilibrium association constant, K_a (reciprocal of K_d), on $1/T$ for the binding of HEWL and HSA onto immobilised Cibacron Blue F3G-A, IDA–Cu^{2+} and polyaspartic

Table 7
The q_m, K_d and η values derived for a single-component Langmuir- or Freundlich equilibrium binding process obtained for the interaction of HEWL with polyaspartic acid immobilised onto Fractosil 1000, with an average particle diameter of 63–100 μm, at different temperatures

Polyaspartic acid immobilised	q_m (mol^{-1})$\times 10^{-7}$ g^{-1}		K_d (M)$\times 10^{-5}$,	η
onto Fractosil 1000	Langmuir	Freundlich	Langmuir	Freundlich
HEWL (4°C)	40.9	38.3	0.19	0.175
HEWL (15°C)	32.2	26.4	0.52	0.172
HEWL (25°C)	30.6	24.9	0.58	0.174
HEWL (37°C)	35.3	30.6	0.32	0.174

The experimental data were fitted to the Eq. (3) and 4 according to the procedures described in the Materials and Methods section

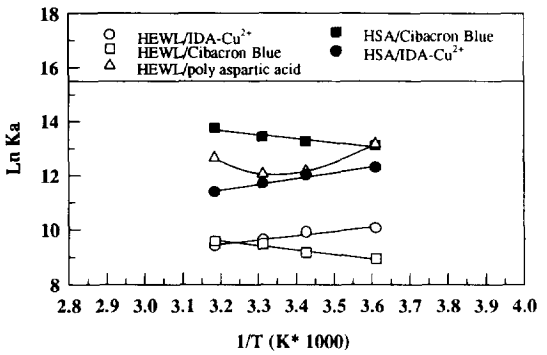

Fig. 15. Van 't Hoff plots for the adsorption of lysozyme and HSA to different functional ligands immobilised onto Fractosil 1000 at the same ionic strength.

acid immobilised onto Fractosil 1000 was analysed in terms of Van't Hoff plots (Fig. 15). For both HEWL and HSA, essentially linear dependencies were observed with both the immobilised dye and the immobilised metal ion chelate ligands, whilst the slope of the plots suggested that the apparent change in the enthalpy of association of both proteins with the respective immobilised dye and immobilised metal ion ligands was independent of temperature. Deviation from linearity was observed in the Van't Hoff plot of log K_a versus $1/T$ for the interaction of HEWL with the immobilised polyaspartic acid ligands. This interactive behaviour is probably due to a predominant contribution to the protein–ligand interaction from coulombic forces at lower temperatures and more significant contributions from hydrophobic forces at higher temperatures, i.e., different protein conformational states at different temperatures may lead to the accessibility of a larger number of hydrophobic amino acid residues that can participate in the interaction with this polymer-like ligand-coating of the Fractosil 1000.

3.6.1. Changes in apparent free energy

The ΔG_{assoc} values for HEWL and HSA adsorbed onto Cibacron Blue F3G-A, IDA–Cu^{2+} and polyaspartic acid immobilised onto Fractosil 1000, respectively, were calculated for each temperature. In accordance with adsorption being a favourable process, the derived ΔG_{assoc} values, tabulated in Tables 8–12, were all negative, i.e. the different ΔG_{assoc} values obtained for the proteins used in these investigations ranged from −4.92 to −7.02 kcal mol^{-1} (1 cal = 4.184 J). These values are of similar magnitude to those obtained by Hutchens and Yip [39] in their study of the binding of several proteins onto immobilised IDA–Cu^{2+} Sepharose Fast Flow, where, for example, a value of $\Delta G_{assoc} = -6.2$ kcal mol^{-1} at all temperatures was obtained for the binding of HEWL.

Table 8
Change in the apparent free energy (ΔG_{assoc}) and entropy (ΔS_{assoc}) for the binding of HEWL at different temperatures to Cibacron Blue F3G-A immobilised onto Fractosil 1000

Temperature (K)	ΔG_{assoc} (kcal mol^{-1})	ΔS_{assoc} (cal mol^{-1} degree)
277	−4.92	5.05
288	−5.25	5.09
298	−5.61	7.02
310	−5.91	7.69

The value of the change in the apparent enthalpy for the interaction of HEWL with this adsorbent was $\Delta H_{assoc} = -3.52$ kcal mol^{-1}.

Table 9
Change in the apparent free energy (ΔG_{assoc}) and entropy (ΔS_{assoc}) for the binding of HSA at different temperatures to Cibacron Blue F3G-A immobilised onto Fractosil 1000

Temperature (K)	ΔG_{assoc} (kcal mol^{-1})	ΔS_{assoc} (cal mol^{-1} degree)
277	−7.21	14.1
288	−7.59	14.9
298	−7.95	15.6
310	−8.47	16.7

The value of the change in the apparent enthalpy for the interaction of HSA with this adsorbent was $\Delta H_{assoc} = -3.31$ kcal mol^{-1}.

Table 10
Change in apparent free energy (ΔG_{assoc}) and entropy (ΔS_{assoc}) for the binding of HEWL at different temperatures to IDA–Cu^{2+} immobilised onto Fractosil 1000

Temperature (K)	ΔG_{assoc} (kcal mol^{-1})	ΔS_{assoc} (cal mol^{-1} degree)
277	−5.54	32.5
288	−5.67	31.7
298	−5.71	30.8
310	−5.80	29.9

The change in the apparent enthalpy for the interaction of HEWL with this adsorbent was $\Delta H_{assoc} = 3.46$ kcal mol^{-1}.

Table 11
Change in the apparent free energy (ΔG_{assoc}) and entropy (ΔS_{assoc}) for the binding of HSA at different temperatures to IDA–Cu^{2+} immobilised onto Fractosil 1000

Temperature (K)	ΔG_{assoc} (kcal mol^{-1})2	ΔS_{assoc} (cal mol^{-1} degree)
277	−6.77	41.6
288	−6.87	40.3
298	−6.93	39.2
310	−7.02	37.9

The value of the change in the apparent enthalpy for the interaction of HSA with this adsorbent was $\Delta H_{assoc} = 4.74$ kcal mol^{-1}.

3.6.2. Changes in apparent entropy

The apparent ΔS_{assoc} values for the binding of HEWL and HSA to Cibacron Blue F3G-A, IDA–Cu^{2+} and polyaspartic acid immobilised, respectively, onto Fractosil 1000 are shown in Tables 8–12. As noted above, these ΔS_{assoc} values should be considered as apparent, since the phase ratio (R_v), i.e., the ratio of the volume of stationary phase to mobile phase in the finite bath, is also dependent on temperature. At lower temperatures, due to the higher viscosity and lower kinetic motion of the ligands, the value of the phase ratio will be different to that at higher temperatures and this difference will impact on the values of the respective thermodynamic ΔS_{assoc} parameters. Positive values for the apparent ΔS_{assoc} were obtained in all cases, indicating an increase in the total disorder of the system during adsorption. The origin of these changes in the apparent ΔS_{assoc} for the process could be due to a combination of solvent dissociation events, a change in conformation of the protein when bound to the adsorbent compared to when free in solution and changes in the relative ordering of the ligands. It was noteworthy that the value of the apparent ΔS_{assoc} for the HSA–Cibacron Blue F3G-A-immobilised Fractosil 1000 interaction was three times that for the HEWL–Cibacron Blue F3G-A-immobilised Fractosil 1000 system. If the change in protein conformation and the ordering/disordering of solvent molecules were the only factors affecting the change in entropy of the association process, the apparent ΔS_{assoc} values should have been within the same range, when the same protein was bound onto different adsorbents. This is clearly not the case, with the experimental data showing a greater value for the change in apparent ΔS_{assoc} for the adsorption of HEWL onto immobilised IDA–Cu^{2+}–Fractosil 1000 than onto immobilised Cibacron Blue F3G-A–Fractosil 1000. The change in state of the ligand before and after the protein has bound thus represents an important contributor to the apparent ΔS_{assoc} values with these silica-based, and presumably other classes of, adsorbents.

Table 12
Change in the apparent free energy (ΔG_{assoc}) and entropy (ΔS_{assoc}) for the binding of HEWL at different temperatures to polyaspartic acid immobilised onto Fractosil 1000

Temperature (K)	ΔG_{assoc} (kcal mol^{-1})	ΔS_{assoc} (cal mol^{-1} degree)
277	−5.03	9.4
288	−5.32	10.0
298	−5.92	10.6
310	−5.92	11.3

3.6.3. Changes in apparent enthalpy

Tables 8–12 list the calculated values for the change in the apparent enthalpy of the association (ΔH_{assoc}) for the interaction for the two proteins with different immobilised ligand systems. As evident from these data, changes in the apparent ΔH_{assoc} were small, and for the immobilised dye affinity and polyaspartic acid adsorbents typically were within the range of −3.52 to −4.74 kcal mol^{-1}. Since the change in the apparent enthalpy of association for the adsorption of HSA and HEWL onto immobilised Cibacron Blue F3G-A–Fractosil 1000 (as well as the immobilised polyaspartic acid Fractosil 1000) was negative, these results indicate that both HEWL and HSA are more prone to be adsorbed onto immobilised Cibacron Blue F3G-A at higher temperature, a finding consistent with the increased contribution from hydrophobic effects at higher temperatures. Change in the apparent ΔH_{assoc} will include contributions from the energy of bringing two surfaces together (Van der Waals forces) and the enthalpy of desolvation and/or resolvation of the solute and the interactive surfaces of the ligand upon adsorption. From the experimental results, it can also be concluded that the binding of the respective proteins to IDA–Cu^{2+} immobilised onto Fractosil 1000 is mainly driven by a positive change in the apparent ΔS_{assoc} of the association process. In the case of this IMAC

system, the value of the apparent ΔH_{assoc} was small and positive. Overall, with the different types of adsorbents, the small changes in the apparent ΔH_{assoc} values indicate that the entropic contributions largely dominate the interaction process at the different temperatures.

4. Conclusions

The results of this investigation have provided further insight into the nature of the adsorption processes of proteins with a range of different silica-based adsorbents. The validity of two isothermal models to appropriately anticipate the experimental findings was also examined. Since the application of methods of isothermal analysis can be used to yield useful information about the maximum capacity and the dissociation constants of a specified protein, equilibrium binding approaches provide a relatively straightforward procedure for acquiring essential data, examining variations in the isothermal behaviour of proteins with different adsorbents in response to changes in temperature, buffer composition or pH, prior to initiating studies with packed- or expanded-bed systems. In subsequent papers, the applicability of these data with frontal analysis procedures with the packed- and fluidised column will be described, providing a direct comparison between adsorption behaviour in a well-stirred tank, a packed-bed and an expanded-bed column.

Acknowledgments

These investigations were supported by the Australian Research Council. G.M.S. Finette was a recipient of a PIRA-Centre for Bioprocess Technology Graduate Scholarship, whilst M.T.W. Hearn wishes to acknowledge the receipt of an Alexander von Humboldt (AvH) Forschungspreis.

References

[1] Q.M. Mao and M.T.W. Hearn, Biotechnol. Bioengin., 52 (1996) 1–19.
[2] A. Jungbauer, J. Chromatogr., 639 (1993) 3–16.
[3] J.C. Janson and P. Hedman, Biotechnol. Prog., 3 (1987) 9–13.
[4] A.W. Purcell, M.I. Aguilar and M.T.W. Hearn, J. Chromatogr. A, 711 (1995) 61–70.
[5] H. Lakhiari, E. Legendre, D. Muller and J. Jozefonvicz, J. Chromatogr. B, 664 (1995) 163–173.
[6] B.E. Boyes and J.J. Kirkland, Pept. Res., 6 (1993) 249–58.
[7] S.A. Lopatin and V.P. Varlamov, Prekl Biokhim Mikrobiol., 31 (1995) 259–66.
[8] W. Kopaciewicz, S. Fulton and S.Y. Lee, J. Chromatogr., 409 (1987) 111–124.
[9] R.M. Chicz, Z. Shi and F.E. Regnier, J. Chromatogr., 359 (1986) 121–130.
[10] F.B. Anspach, H.-J. Wirth, K.K. Unger, P.G. Stanton, J.R. Davies and M.T.W. Hearn, Anal. Biochem., 179 (1989) 171–181.
[11] A.J. Alpert, J. Chromatogr., 266 (1983) 23–37.
[12] D.A.P. Small, A. Atkinson and C.R. Lowe, J. Chromatogr., 266 (1983) 151–156.
[13] I. Langmuir, J. Am. Chem. Soc., 40 (1918) 1361–1403.
[14] B.J. Horstmann, C.N. Kenney and H.A. Chase, J. Chromatogr., 361 (1986) 179–190.
[15] F.B. Anspach, A. Johnston, H.-J. Wirth, K.K. Unger and M.T.W. Hearn, J. Chromatogr., 476 (1989) 205–225.
[16] H. Yoshida and T. Kataoka, Chem. Eng. J., 41 (1989) 11–15.
[17] H. Freundlich, Z. Physik. Chem., 57 (1907) 385–470
[18] S. Jacobson, S. Golshan-Shirazi and G. Guiochon, AIChE J., 37 (1991) 836–844.
[19] J. Jain and V.L. Snoeyink, J. Water Pollut. Contr. Fed., 45 (1973) 2463–2479.
[20] J.A. Butler and C.J. Ockrent, Phys. Chem., 34 (1930) 2841–2859.
[21] R.H. Fowler and E.A. Guggenheim, Statistical Thermodynamics. Cambridge University Press, Cambridge, 1939.
[22] G. Oddie and M.T.W. Hearn, in preparation.
[23] P.A. Belter, F.L. Cunningham and J.W. Chen, Biotechnol. Bioengin., 15 (1973) 533–549.
[24] N.F. Kirkby, N.K.H. Slater, K. Weisenberger, F. Addo-Yobbo and D. Doulia, Chem. Eng. Sci., 41 (1986) 2005–2016.
[25] J.D. Andrade, in J.D. Andrade (Editor), Surface and Interfacial Aspects of Biomedical Polymers, Vol. 2, Plenum Press, New York, 1985.
[26] J. Wei and M.T.W. Hearn, Anal. Biochem., 242 (1996) 44-54.
[27] H.J. Wirth, K.K. Unger and M.T.H. Hearn, Anal. Biochem., 208 (1993) 16–25.
[28] R.C. Travers and F.C. Church, Int. J. Peptide Prot. Res., 26 (1985) 539–549.
[29] E.S. Hemdan, Y.-J. Zhao, E. Sulkowski and J. Porath, Proc. Natl. Acad. Sci. USA, 86 (1989) 1811–1815.
[30] M. Belew, T.T. Yip, L. Andersson and J. Porath, J. Chromatogr., 403 (1987) 197–206.
[31] M. Zachariou, I. Traverso, L. Spiccia and M.T.W. Hearn, J. Phys. Chem., 100 (1996) 12680–12690.
[32] P.M. Boyer and J.T. Hsu, Biotech. Tech., 4 (1990) 61–66.

[33] M.T.W. Hearn, in J.A. Asenjo (Editor), Separation Processes in Biotechnology, Marcel Dekker, New York, 1990, pp. 17–66.
[34] P.M. Boyer and J.T. Hsu, Chem. Eng. Sci., 47 (1992) 241–251.
[35] G.M.S. Finette, Q.M. Mao and M.T.W. Hearn, J. Chromatogr. A, 743 (1996) 57.
[36] F. Qadri and P.D.G. Dean, Biochem. J., 191 (1980) 53–62.
[37] L. Kagedal, in J.C. Janson and L. Ryden (Editors), Protein Purification, VCH, Weinheim, 1989.
[38] F.H. Arnold and H. Blanch, J. Chromatogr., 355 (1986) 13–27.
[39] T.W. Hutchens and T.T. Yip, J. Inorg. Biochem., 42 (1991) 105–118.
[40] R.E. Canfield, J. Biol. Chem., 238 (1963) 2698–2707.
[41] J.R. Brown, Fed. Proc., 35 (1976) 2141–2144
[42] F.W. Fang, M.I. Aguilar and M.T.W. Hearn, J. Chromatogr. A, 729 (1996) 49–66.
[43] M. Zachariou, I. Traverso, L. Spiccia and M.T.W. Hearn, Anal. Chem., submitted.